Nanoscale Res Lett (2009) 4:1171–1177
DOI 10.1007/s11671-009-9378-7

NANO EXPRESS

A Facile Strategy for In Situ Core-Template-Functionalizing Siliceous Hollow Nanospheres for Guest Species Entrapment

Jun Wang · Xin Gao · Xianyan Yang · Yilai Gan · Wenjian Weng · Zhongru Gou

Received: 9 February 2009 / Accepted: 15 June 2009 / Published online: 27 June 2009

Abstract The shell wall-functionalized siliceous hollow nanospheres (SHNs) with functional molecules represent an important class of nanocarriers for a rich range of potential applications. Herein, a self-templated approach has been developed for the synthesis of in situ functionalized SHNs, in which the biocompatible long-chain polycarboxylates (i.e., polyacrylate, polyaspartate, gelatin) provide the framework for silica precursor deposition by simply controlling chain conformation with divalent metal ions (i.e., Ca^{2+}, Sr^{2+}), without the intervention of any external templates. Metal ions play crucial roles in the formation of organic vesicle templates by modulating the long chains of polymers and preventing them from separation by washing process. We also show that, by in situ functionalizing the shell wall of SHNs, it is capable of entrapping nearly an eightfold quantity of vitamin Bc in comparison to the bare bulk silica nanospheres. These results confirm the feasibility of guest species entrapment in the functionalized shell wall, and SHNs are effective carriers of guest (bio-)molecules potentially for a variety of biomedical applications. By rationally choosing the functional (self-templating) molecules, this concept may represent a general strategy for the production of functionalized silica hollow structures.

J. Wang · X. Gao · X. Yang · Y. Gan · Z. Gou (✉)
Zhejiang California International NanoSystems Institute, Zhejiang University, Huajiachi Campus, 310029 Hangzhou, China
e-mail: zhrgou@zju.edu.cn

W. Weng
Department of Materials Science and Engineering, Zhejiang University, Yuquan Campus, 310027 Hangzhou, China

Keywords Self-template · In situ functionalizing shell wall · Guest molecule entrapment · Siliceous hollow nanospheres

Introduction

Inorganic hollow or porous micro-/nanostructures are of great interest in many current and emerging areas of technology partly because of their hollow or porous chamber, high specific surface area, low toxicity and low effective density [1–4]. Such hollow or porous capsules can pave the way for industrial, environmental, biomedical and biotechnological applications such as catalysis, separation, delivery, immobilization and so on [5–8]. Recently, the number of biologically active proteins, drugs and antimicrobials used to treat/prevent disease is growing rapidly, but appropriate inorganic carriers for introduction of these therapeutics into body are often lacking [9–11]. Silica nanoparticles (i.e., bulk, hollow and porous structure) are nontoxic, bioresorbable matrix as versatile carriers and polishing component of toothpastes primarily due to the fine thermal stability and chemical inertia [12–18]. In particular, biomedical and biotechnological applications with siliceous hollow nanospheres (SHNs) are currently focused on guest (bio-)molecules delivery and controlled release. Basically, these applications require the functionalized shell wall with biocompatible functional molecules to effectively improve the loading density of guest species, which would also endow them with diverse properties. Among the various hollow particles production techniques, the template route has been investigated most extensively due to its flexibility in controlling the particles size from micrometer- to nanometer scales [19, 20]. Although the classical sol–gel processes result in SHNs by using the

core-template of micelles and rigid particles [12, 19–21], the synthetic procedures are multistep and complex, and the SHNs have significant shortcomings that limit their functionality in the silica shell as sacrificing templates by either calcination or chemical dissolution. So far, several efforts have been directed toward the structural organization of organic–inorganic hybrid SHNs via the catalytic activity of polymers or vesicle template, but they suffer from potential biocompatibility and ill-defined morphology problems [22–25]. Thus, it is highly desired to develop facile synthesis pathway for SHNs formation with shell wall functionalization for biomedical applications.

The DNA conformational changes, such as nanoscale toroid, spheroid and rodlike structure, modulated by multivalent cations (MVCs) have been widely appreciated as superb model system for understanding gene packing in biological systems [26–28]. This process prompts a number of analogous studies on coils conformation and inorganic superstructure formation by templating of ions-initiating semiflexible polyelectrolyte polymers [29–34]. Particularly, recent studies of DNA template synthesis have also revealed that the 'cationic' plasmid DNA form can act as an attractive template for the formation of ordered circular and rodlike silica nanostructures [35]. We hypothesize that the metal ions (for example, alkaline earth metals) are able to crosslink long-chain polyanionic molecules to form specific morphology with more complexity in comparison with DNA toroid. Thus, a new strategy for constructing a spherical complex (for example, vesicle) using a wide range of polymers for templating SHNs formation has been awaited.

On the basis of these considerations, we have developed a one-step synthesis of biologically friendly SHNs with functionalized hollow chamber from polymers self-templated pathway, thanks only to electrostatic interaction between *polycarboxylates* and *divalent metal ions*. The SHNs are synthesized by a sonochemically assisted wet chemical reaction, and metal ions are used as polymer conformation modulators, without the intervention of any external templates and potentially toxic surfactants or mediums. Specifically, polyacrylate, polyaspartate and alkaline-processed gelatin molecules containing COO^- groups are initially selected because of their biocompatible and noninflammatory nature, and especially because of their reversible conformation changes with small external pH changes [33, 36, 37]. To our knowledge, this is the first report on the mild synthesis of hollow spheres composed of silica shell wall, which is simultaneously (in situ) functionalized by templating biocompatible polymers under the modulation of biologically essential metal ions in aqueous medium.

Experimental

Materials and Reagents

All chemicals used were commercially available. Reagents used for the synthesis of hollow silica nanospheres included tetraethoxysilane (TEOS), absolute ethanol (99.7%), calcium nitrate ($Ca(NO_3)_2{\cdot}4H_2O$, 99.5%), strontium nitrate ($Sr(NO_3)_2{\cdot}4H_2O$, 99.5%), aqueous ammonia (28 wt%) were purchased from Shanghai Chemical Reagent Co. (SCRC, China) and used as received. The polyacrylate sodium (30 wt%, average M_w ~2.5 KDa) (abbreviated as PAS2.5) and poly(aspartic acid) (30 wt%, average M_w ~5.0 KDa) (abbreviated as PAsp5), gelatin (alkalic-processing; 10 wt%, average M_w ~75 KDa) were obtained from SCRC. Deionized distilled water (DDW) was used throughout the experiment.

Synthesis of Siliceous Hollow Nanospheres

In a typical procedure, for instance of experiment No. 1 as mentioned in Table. 1, 1.0 ml of PA (30 wt%, M_w 2.5 KDa, denoted as PA2.5), 0.5 ml of $Ca(NO_3)_2$ solution (0.5 M) and 2.2 ml of ammonia (28%) were added to 26.2 ml of DDW and magnetically stirred for 10 min, after which 20 ml of ethanol (99.7%) was added sequentially to the aqueous solution and stirred for 5 min. The resulting solution was subsequently added into a 200-ml three-necked flask with a mechanical stirrer, in a water bath of ultrasonic (US) generator (40 kHz, 80 W). Then 1.6 ml of TEOS was added into 50 ml of ethanol under stirring for 1 min to ensure complete mixing. Immediately, the mixture was also added into the flask under vigorous stirring and ultrasonicating. The white powders obtained by three-repeated centrifugation/DDW-wash cycles at scheduled time and dried in vacuum. Similarly, the synthesis was taken by using $Sr(NO_3)_2$ as the dicationic inducer (The strontium ions is one of the important biologically active trace elements). The similar synthesis procedure was also taken as controls without and with acoustic cavitation in the presence and absence of divalent metal ions, as mentioned in Table. 1, No. 2 and 3. To understand the structure variation, more SHNs were synthesized by only changing the PAsp5 or gelatin template under the same initial pH condition (Table. 1, No. 4 and 5). In addition, the so-called *pure* bare bulk silica nanospheres with solid-core were also prepared in the absence of both organic additives and metal ions, while the other reaction conditions remained the same (Table. 1, No. 6).

Table 1 Synthesis details and conditions for the preparation of silica nanospheres

Series	Polymer[a]	Divalent metal ion	Ultrasonication[b]	Ageing time (min)	Microstructure[c]
No. 1	PA2.5	Ca or Sr	US	5, 12, 20	Hollow
No. 2	PA2.5	Ca or Sr	No US	20	Hollow and bulk
No. 3	PA2.5	–	US	20	Bulk
No. 4	PAsp5	Ca or Sr	US	20	Hollow
No. 5	Gelatin	Ca or Sr	US	20	Hollow
No. 6	–	–	No US	20	Bulk

[a] PA2.5: M_w ca. 2.5 KDa, 30 wt%; Getalin: M_w ca. 75 KDa, 10 wt%; PAsp5: M_w 5.0 KDa, 30 wt%

[b] The reactions with and without the assistance of ultrasonication (US) condition were denoted as US and no US, respectively

[c] The microstructures of silica particles were characterized by using transmission electron microscopy

Examination of the As-Synthesized SHNs as a Carrier of Biomolecules

The 0.8 wt% Vitamin Bc (denoted as VB, KCl solution, pH = 10.5) and the freshly as-synthesized SHNs were mixed in a suspension with the weight ratio of VB/SHNs = 1/2, which was stirred vigorously for 8 h. After rinsed with KCl solution (pH = 10.5) to remove the un-entrapped molecules, the powders with the entrapped VB dried in vacuum. As a comparison of the test on entrapment efficiency, the experiment of bare bulk silica nanospheres (100 nm or less in diamater) entrapping VB was taken as control.

Characterization

The dried powders were determined by X-ray diffraction (XRD, Rigaku D/max-rA) with Cu Kα radiation at a scanning rate of 0.01°/min and Fourier transform Infrared (FTIR, Nicolet) for the phase composition. The morphology and chemical composition of the particles were determined by transmission electron microscopy (TEM, JEOL JEM-2010) connected with energy-dispersive X-ray analysis (EDX, INCA EDAX, element > B) operating at 200 kV. The scanning electric microscopy (SEM) images were taken on a JEOL JEM-6700F microscope. Samples were deposited onto quartz slides. Thermo-gravimteric analysis (TGA) was performed using a TG/DTA6200, with heating rate of 10 °C min^{-1} in air. All the samples were washed with DDW and dried to remove the physicosorbed polymers prior to analysis.

Results and Discussion

We hypothesize that divalent metal ions (i.e., alkaline earth metals) crosslink long-chain polymers to form vesicle-like geometry, similar to DNA toroid under the mediation of multivalent cation. The synthesis conditions for the siliceous nanoparticles can be seen from Table 1. The transmission electron microscopy (TEM) and scanning electron microscopy (SEM) images in Fig. 1a and b show that when

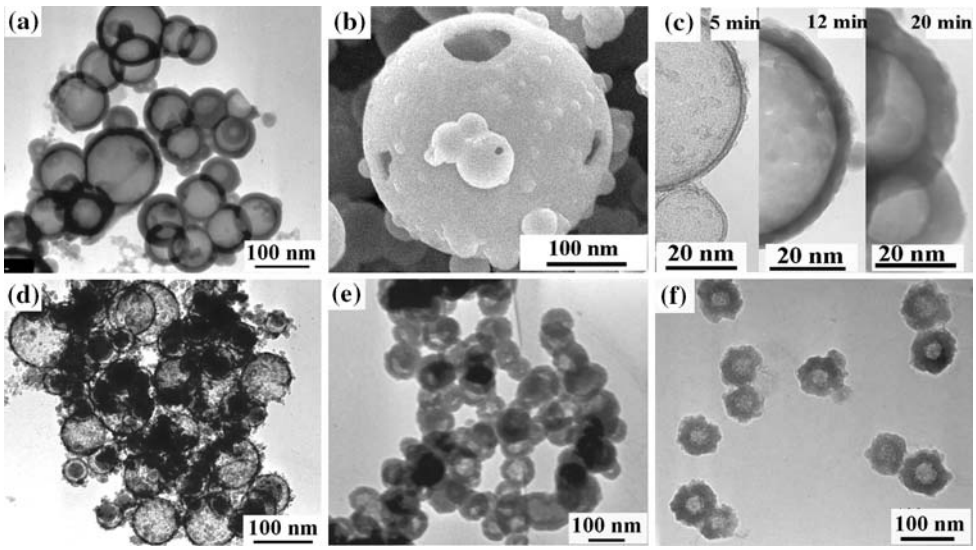

Fig. 1 TEM and SEM images of SHNs mediated by PA2.5 with (**a**–**c**) and without (**d**) cavitation, PAsp5 with cavitation (**e**), gelatin with cavitation (**f**)

PA2.5 and Ca^{2+} ions were used as structural templates (No. 1, Table. 1), the particles exhibit hollow interiors, spherical particle morphology, small opens and nanometer-scale dimension. The diameters of the SHNs are approximately 200 nm or less. The shell wall growth process was monitored by TEM. TEM imaging of the shell wall is shown Fig. 1c, which contains representative images. As expected, the shell thickness (4–20 nm), estimated by high magnification images from ring around the perimeter of hollow structure, could be precisely tailored through prolonging the reaction time (5–20 min), suggesting that the silica precursors continuously deposit onto the shell wall surface. Another prominent feature of the SHNs is that there are several open holes in the shell walls (Fig. 1b). These porous structures with openings of over 10 nm in diameter, larger than the mesoporous cavities of silica particles, are enough to accommodate the guest macromolecules, and thus tend to be much easily immobilized and released, without destructing the chamber of the SHNs [38]. This is likely due to the durative cavitation stimuli so that small openings are necessary to maintain the pressure balance between the inside and outside of shell walls. Furthermore, this unique method using the other polycarboxylate and divalent metal ions mixtures as templates can be extended to synthesize similar hollow nanoparticles. Figure 1e and f illustrates the resulting SHNs with a rather uniform diameter and shell thickness through using the PAsp5 and gelatin as core templates (No. 4 and 5, Table 1). It is worth noting that a control experiment (No. 2, Table 1) without sonication did show the evidence of hollow nanostructure, though a few bulk particles were observed (Fig. 1d). However, the similar suspension in the presence of polymers but in the absence of metal ions (No. 3, Table 1), yielded bulk silica nanoparticles, which is almost the same as that harvested from the conventional stöber method (No. 6, Table 1). It is clear that the structure-directing metal ions induce the formation of vesicle in this process, which is partly supported by the experimental results of Schweins et al. [31] and Göransson et al. [32] that a long-chain polymer and oppositely charged surfactant/ions mixture solution with different mole ratios induce the formation of vesicles in a sufficiently diluted NaBr or NaCl solution. Therefore, the diverse experimental results clearly suggest the long-chain polycarboxylate templates mediated by divalent metal ions in the silica precursor aqueous medium enable the production of siliceous hollow shell morphology.

Figure 2 shows the EDX spectrum that revealed that the SHNs were indeed composed of silica (Si, 71.99 wt%), metal ion (Ca, 0.30 wt%) and polymers (C, 3.12 wt%). However, it is difficult to determine the accurate content of polymers on the basis of the EDX spectrum, since element C from carbon film supported on the copper grid has been

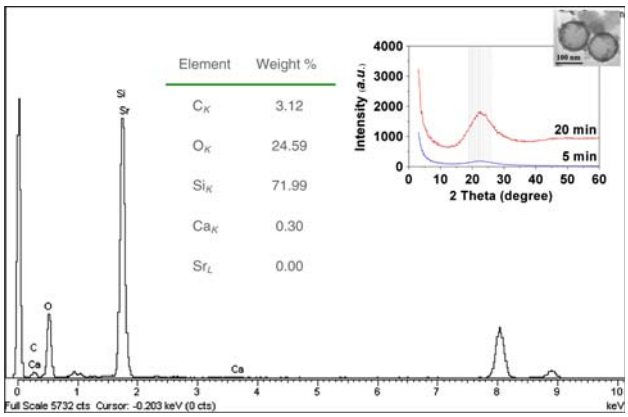

Fig. 2 EDX spectrum of SHNs synthesized by using PA2.5 and calcium ions with a 20 min of ageing time. The sample was thoroughly washed with DDW at 37 °C to remove the organic molecules physicosorbed on the surface of hollow spheres prior to analysis. In the *inset* XRD patterns of SHNs exhibiting different intensities at 22°–26°/2θ with the prolongation of ageing time are displayed

included. Additionally, X-ray diffraction (XRD) measurement shows the grown peaks in the silica region at ~22°–26°/2θ with progression in the deposition and maturation process (from 5 to 20 min). The amorphous nature was confirmed by the diffused wide patterns from the XRD data (inset, Fig. 2).

It also highlighted the importance of the shell wall modification to entrap guest molecules. Fourier-transformed infrared (FTIR) spectra are shown in Fig. 3. As expected, the absorption bands at 1,660–1,400 cm^{-1} corresponding to the amide I (C=O/C–N stretch) and II (N–H bend/C–H stretch) of PAsp5 or carboxylic group (C=O stretch) of PA2.5 were observed. However, this is different to the bare hollow silica free from the organic additives synthesized in a W/O/W emulsion system [39]. This suggests that the metal ions act as

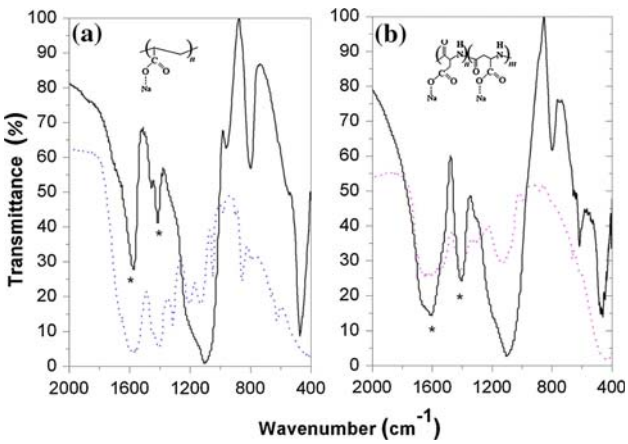

Fig. 3 FTIR spectra (*solid lines*) of the SHNs synthesized in the presence of PA2.5 (**a**) and PAsp5 (**b**), respectively. The *dot lines* represent the FTIR spectra of pure PA2.5 and PAsp5, respectively

bond bridges between functional molecules and silanol groups so that the polymers exhibit very well washing-resistant ability, in comparison to the compact aggregated polymer templates sensitive to washing process [14]. Evidently, the polymer spherical geometry (just as "soft" template) substantially represents a fundamental morphology selected by the spatial charge stability in solution, which is similar to the observed DNA toroidal compaction, but distinct from the polymer-silica hybrid films or spheres under slightly acidic condition [40, 41]. Furthermore, although the structure-directing metal ions are readily attached on the surface of the polymer vesicles through electrostatic interaction with side carboxylic groups, the excessive dications possibly reside within the silica shell/medium interfacial region and contribute to a decrease in electrical double layer, avoiding silica nucleation in the suspension. Throughout the experiment, the structure of the vesicles does not collapse during the sol–gel process of silica sources, which result in the silica shell completely replicating the vesicle's structure, and the shell thickness increase rapidly.

Another important point, however, that has not been studied in previous reports is the loading capability for guest species of the SHNs obtained after washing process. In order to determine whether guest molecules can be entrapped by the shell chambers of the as-synthesized SHNs, in vitro adsorption experiments were conducted. Specifically, the measure of entrapment efficacy was obtained by using Vitamin Bc (VB) as model molecule and verified by TGA (Fig. 4). VB, folic acid, and other names of the same chemical, long believed to be of great medicinal benefit, is composed of a pteridine nucleus, a pteroyl portion and glutamic acid and is coenzyme

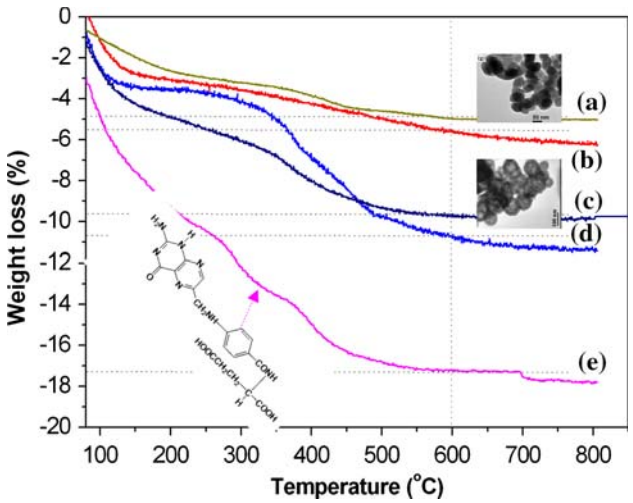

Fig. 4 Thermogravimeteric analysis (TGA) of the SHNs and bulk silica nanoparticles before and after entrapping VB. **a** bulk Silica nanoparticles, **b** VB-entrapped bulk silica nanoparticles, **c** SHNs synthesized in the presence of PA2.5, **d** SHNs synthesized in the presence of PAsp5, **e** VB-entrapped SHNs

involved in transfer and utilization in a variety of essential physiological reactions, including amino acid metabolism, biosynthesis of DNA and RNA and prominent antitumor activity [42, 43]. By contrast with the bulk silica (curve *a*), the added weight loss between 250 and 600 °C of 4.9 and 5.7% under the background level of curve *b* corresponded to thermolysis of PA2.5 (curve *c*) and PAsp5 (curve *d*), respectively. More interestingly, a clear distinction between bulk and hollow spheres afterward internalizing VB could be measured by TGA. The weight loss increased drastically ($\sim$6.5%) after entrapping VB (compare curve *d* with *e*), which was predominantly associated with the thermolysis of VB. In contrast, the weight loss of bulk silica changed little (<0.8%) before and after entrapping VB (compare curve *a* with *b*), implying a strong dependence of the trapping efficiency of gust molecules on surface functionality. It should be noted, however, that since VB internalized in hollow chamber were more difficult to volatilize than those adsorbed on the bulk silica surface, the volatilization of VB underwent a wide temperature range. There is more than an eightfold obvious increase in the VB-entrapped quantity versus those on the bare bulk silica nanospheres. This increase is attributed to caging effects that isolate VB from the aqueous medium and from specific strong interactions. This is possibly helpful to develop new bioactive molecule delivery system for therapeutic and antimicrobial applications.

More recently, other authors have also reported that block copolymer micelle initialized in chloroform, besides the cationic DNA circular or coiled-coil structures [35], can act as morphologically changeable templates for hollow silica spheres or tubules formation [44]. Indeed, we agree when these aggregated polymer micelle is viewed as template for SHNs, in which the terminal amide groups instead of the cationized side groups is the anchor point for silica nucleation. In the present study, we find significant differentiation from the polymer templates in the presence and absence of metal ions, however (for example, those shown in Table.1, No. 1 and No. 3). This phenomenon is evidently deviated from the existing aggregated polymer-templating synthesis with and without the assistance of sonication [14, 15].

A proposed mechanism is displayed in Scheme 1 showing the electrostatic interaction between organic molecules and metal ions and subsequently similar interaction between metal ions and silanol groups of silica precursor. Generally, the long-chain polycarboxylate with a large quantity of electron-donating side groups (COO^- groups) itself is expanded by electric repulsion according to the dissociation of the ionic groups in a dilute basic solution [45] (Scheme 1 a, b). When the dications (i.e., Ca^{2+}, Sr^{2+}) are added into the solution, the carboxylic side groups of the polymers interact electrostatically or chelate

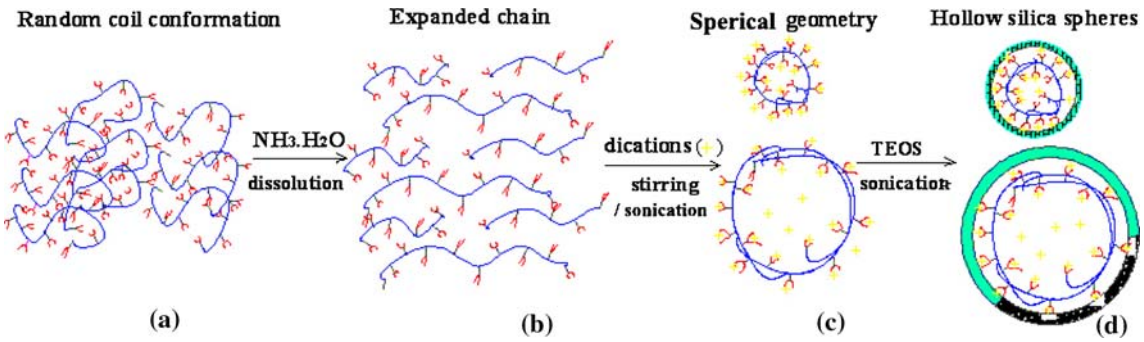

Scheme 1 Schematic representation of the long-chain polymer vesicular self-templating SHNs formation, and in situ functionalized with biocompatible polymer, rich in side carboxylic acid

with the dications. Then, the main-chains of the polymers bend and pack into a spherical vesicle-like geometry with an appropriate size of ~100 nm in diameter under the assistance of sonication (Scheme 1b, c). Accordingly, the side carboxylic chains anchored with metal ions may be favorable for interacting with the negatively charged silica precursors (Scheme 1c, d), and well-defined spherical morphology of silica shell architectures produced on the polymer vesicle.

In addition, our many check and reproducible experiments, for example the "cationic" polyepoxysuccinate vesicles, validated the SHNs production while the other reaction conditions remained the same (data not shown). It is obvious that the side-chain complexity of polyacrylate, polyaspartate and gelatin is increased progressively. The alkalic-processed gelatin, formed from denatured and degraded collagen, has a poorly defined structure, but the portions of collagen molecules with characteristic triple helical structure are still present and lie in parallel layers. Thus, this molecule possesses a great proportion of carboxyl groups, rending it negatively charged and expanding in the alkaline aqueous solution.

Conclusions

In summary, we have developed a more facile and versatile method to obtain highly functionalized HSNs with openings. The shell wall thickness of the hollow spheres can be easily tailored by varying the aging time, and the particle size can be controlled below submicron dimension. This method is based on the in situ adsorption of functional molecules in the hollow chamber of hollow spheres in an aqueous medium, without involving additional template and hazardous additives. The participation of electrostatic interactions between a diversity of carboxylic groups-rich long-chain polymers and divalent metal ions was evidenced. Extension of the present versatile technique to other functional polymers may enable the preparation of siliceous hollow carriers with different functionalities. These materials with high functionalized shell wall could be good candidates for guest molecules adsorption, which is particularly useful in the biomolecules delivery for therapy and antimicrobial agent release for preventing caries.

Acknowledgments The authors would like to acknowledge financial support by the FSTDZP (2008C21058), CFZUWST (H20080039) and ZCNI (J30802).

References

1. D.L. Wilcox, M. Berg, T. Bernat, D. Kellerman, J.K. Cochran (Eds.), Hollow and Solid Spheres ans Microspheres. MRS symposium Proceedings. Vol. 372 Materials Research Society, Pittsburg, PA, 1995
2. K.K. Perkin, J.L. Tuner, K.L. Wooley, S. Mann, Nano. Lett. **5**, 1457 (2005)
3. Y. Cai, H. Pan, X. Xu, Q. Hu, L. Li, R. Tang, Chem. Mater. **19**, 3081 (2006)
4. A.M. Collins, C. Spickermann, S. Mann, J. Chem. Mater. **13**, 1112 (2003)
5. M. Lal, L. Levy, K.S. Kim, G.S. He, X. Wang, Y.H. Min, S. Pakatchi, P.N. Prasad, Chem. Mater. **12**, 2632 (2000)
6. K. Sharma, S. Das, A. Maitra, J. Colloid Interface Sci. **284**, 358 (2005)
7. X. Tan, S. Li, J. Membr. Sci. **188**, 87 (2001)
8. J.J.E. Lee, J. Lee, J.H. Yu, B.C. Kim, K. An, Y. Hwang, C.H. Shin, J.G. Park, J. Kim, J. Am. Chem. Soc. **128**, 688 (2006)
9. R. Langer, Nature **392**, 5 (1998)
10. X.W. Lou, L.A. Archer, Z. Yang, Adv. Mater. **20**, 1 (2008)
11. Y. Piao, A. Burns, J. Kim, U. Wiesner, T. Hyeon, Adv. Funct. Mater. **18**, 1 (2008)
12. C. Barbé, J. Bartlett, L. Kong, K. Finnie, H.Q. Lin, M. Larkin, S. Calleja, A. Bush, G. Calleja, Adv. Mater. **16**, 1959 (2004)
13. G. Caturan, R.D. Toso, S. Boninsegna, R.D. Monte, J. Mater. Chem. **14**, 2087 (2004)
14. T. Shiomi, T. Tsunoda, A. Kawai, H. Chiku, F. Mizukami, K. Sakaguchi, Chem. Commun. 5325 (2005). doi: 10.1039/b507736b
15. Y. Wan, S.-H. Yu, J. Phys. Chem. C **112**, 3641 (2008)
16. W. Fan, L. Zhao, J. Colloid Interface Sci. **297**, 157 (2006)
17. D.J. Bharali, I. Klejbor, E.K. Stachowiak, P. Dutta, I. Roy, N. Kaur, E.J. Bergey, P.N. Prasad, M.K. Stachowiak, PNAS **102**, 11539 (2005)

18. R.M. Gaikward, I. Sokolov, J. Dent. Res. **87**, 980 (2008)
19. F. Caruso, R.A. Caruso, H. Mhwald, Science **282**, 111 (1998)
20. M. Chen, L. Wu, S. Zhou, B. You, Adv. Mater. **18**, 801 (2006)
21. Y.J. Wang, F. Caruso, Chem. Mater. **17**, 953 (2005)
22. K.J.C. van Bommel, J.H. Jung, S. Shinkai, Adv. Mater. **13**, 1472 (2001)
23. J.F. Chen, H.M. Ding, J.X. Wang, L. Shao, Biomaterials **25**, 723 (2004)
24. D. Ma, M. Li, A.J. Patil, S. Mann, Adv. Mater. **16**, 1838 (2004)
25. D.H.W. Hubert, M. Jung, P.M. Frederik, P.H.H. Bomans, J. Meuldijk, A.L. German, Adv. Mater. **12**, 1286 (2000)
26. N.V. Hud, I.D. Vilfan, Annu. Biophys. Biomol. Struct. **34**, 295 (2005)
27. W.M. Gelbart, R.F. Bruinsma, P.A. Pincus, V.A. Parsegian, Phys. Today **53**, 38 (2000)
28. N.V. Hud, K.H. Downing, PNAS **98**, 14925 (2001)
29. A. Tsortos, G. Nancollas, J. Colloid Interface Sci. **250**, 159 (2002)
30. F. Molnar, J. Rieger, Langmuir **21**, 786 (2005)
31. R. Schweins, P. Lindner, K. Huber, Macromolecules **36**, 9564 (2003)
32. A. Göransson, P. Hansson, J. Phys. Chem. B **107**, 9203 (2003)
33. B. Fiers, T. Kiefhaber, J. Am. Chem. Soc. **129**, 672 (2007)
34. K. Huber, T. Witte, J. Hollmann, S. Keuker-Baumann, J. Am. Chem. Soc. **129**, 1089 (2007)
35. M. Numata, K. Sugiyasu, T. Hasegawa, S. Shinkai, Angew. Chem. Int. Ed. **43**, 3279 (2004)
36. Y. Zhang, M. Jiang, J. Zhao, Z. Wang, H. Dou, D. Chen, Langmuir **21**, 1531 (2005)
37. G. Tamás, T. Viktória, G. Benjámin, Z. Miklós, Acta Biomater. **4**, 733 (2008)
38. M. Fujiwara, K. Shiokawa, K. Hayashi, K. Morigaki, Y. Nakahara, J. Biomed. Mater. Res. Part A **81A**, 103 (2007)
39. M. Fujiwara, K. Shiokawa, I. Sakakura, Y. Nakahara, Nano. Lett. **6**, 2925 (2006)
40. R. Mouawia, A. Mehdi, C. Reyé, R. Corriu, J. Mater. Chem. **17**, 616 (2007)
41. M. Khiterer, K.J. Shea, Nano. Lett. **7**, 2684 (2007)
42. R.T.P. Paul, A.P. McDonnell, C.B. Kelly, Hum. Psychopharmacol. Clin. Exp. **19**, 477 (2004)
43. S.D. Weitman, R.H. Lark, L.R. Coney, D.W. Fort, V. Frasca, V.R. Zurawski Jr., B.A. Kamen, Cancer Res. **52**, 3396 (1992)
44. H. Lee, K. Char, Appl. Mater. Interfaces **1**, 913 (2009)
45. C. Déjugnat, G.B. Sukhorukov, Langmuir **20**, 7265 (2004)